Materials Advances

ROYAL SOCIETY OF CHEMISTRY

COMMUNICATION

View Article Online
View Journal | View Issue

Check for updates

Cite this: *Mater. Adv.*, 2020, 1, 595

Received 7th May 2020,
Accepted 13th June 2020

DOI: 10.1039/d0ma00286k

rsc.li/materials-advances

Synthesis of heterocyclic aramid nanofibers and high performance nanopaper†

Yifei Shi and Xinlin Tuo *

The construction of heterocyclic aramid nanofibers (HNFs) was reported for the first time in this study by a polymerization-induced self-assembly method. 2-(4-Aminophenyl)-5-aminobenzimidazole was introduced as the third monomer to participate in the polymerization of poly(*p*-phenylene terephthalamide) and HNFs were successfully prepared based on the balance of the solvent isolation effect and intermolecular interaction. Subsequently, HNFs were fabricated into nanopaper, which has uniform micro–nano structures and significantly improved mechanical properties and electrical insulation.

In recent years, aromatic polyamide poly(*p*-phenylene terephthalamide) (PPTA) based nanofibers (ANFs) have become a research hotspot in the field of high performance polymers due to their excellent properties and novel processibility.[1–5] ANFs have broad application prospects in many fields, such as adsorption materials,[6,7] reinforced composites,[8–10] flexible conductors,[11] supercapacitors,[12,13] and infrared stealth materials.[14] So far, there are various methods for preparing ANFs, such as electrospinning, mechanical disintegration and the deprotonation method, but these methods have little industrial production value.[15] Based on the "bottom-up polymerization-induced self-assembly" method for preparing ANFs invented by our group,[5] ANFs can be produced on a large scale and retain the physical and chemical properties of PPTA. However, the preparation of ANFs by this method requires polyoxyethylene ether as an interfacial isolation additive,[5] which could not be thoroughly removed due to covalent or noncovalent bond force and subsequently gives rise to the risk of the performance of ANFs.

One of the most important uses of ANFs is to prepare aramid paper.[16–20] Aramid paper is an essential raw material for the application of high-grade insulation and honeycombs, which strictly requires high performance of ANFs. PPTA-based ANF paper has high tensile strength, great thermal stability and excellent insulation properties.[21] However, because of the rigid molecular chain characteristics of PPTA, ANF paper also exhibits the disadvantage of brittleness and its elongation at break is usually around 5%, showing insufficient toughness.[21] Thus, it is in urgent need to modify ANFs and improve the performance of nanopaper.

Copolymerization has been proved to be an effective strategy to adjust the properties of PPTA.[22–26] Herein, we introduce the heterocyclic monomer 2-(4-aminophenyl)-5-aminobenzimidazole (APBZ) as a third monomer to participate in PPTA polymerization and expect to obtain modified copolymerized nanofibers. Heterocyclic aramid fiber is famous for its better strength and tenacity than PPTA fiber.[27,28] Heterocyclic aromatic polyamides (HAPs) are generally prepared in the dimethylacetamide (DMAc)/LiCl system, which is more conducive to the stability of the synthesized copolymer.[29,30] However, based on the principle of polymerization-induced self-assembly to obtain ANFs, the DMAc/LiCl solvent system is actually not a good choice for the formation of nanofibers. From the perspective of industrial production, it has high cost and complicated aftertreatment. In contrast, the solvent system of *N*-methyl-2-pyrrolidone (NMP)/$CaCl_2$ is less costly, easy to recycle and has excellent interface isolation effect for the PPTA molecular chain.[31,32] The cation of the salts could complex with the carbonyl group of NMP, and the anion could combine with the hydrogen atom on the amide bond of the polymer, thereby isolating the molecular chain and increasing the solubility of the aromatic polyamides. Therefore, in this paper, we expect to prepare heterocyclic aramid nanofibers (HNFs) in the NMP/$CaCl_2$ solvent system without any interfacial additives.

As a result, HNFs were first prepared by copolymerization and then HNF papers with uniform structure, excellent mechanical properties and electrical insulation were also successfully fabricated as shown in Fig. 1. The effect of comonomer addition ratio on the HNF morphology and HNF paper properties was studied briefly. It is important to notice that the modification by copolymerization expands the application range of aramid nanofibers, which is expected to be applied to fields with higher performance requirements.

Key Laboratory of Advanced Materials (MOE), Department of Chemical Engineering, Tsinghua University, Beijing 100084, P. R. China. E-mail: tuoxl@tsinghua.edu.cn

† Electronic supplementary information (ESI) available. See DOI: 10.1039/d0ma00286k

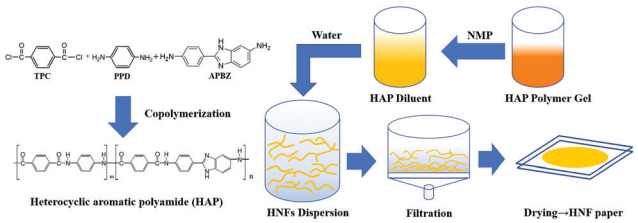

Fig. 1 Schematic process of the preparation of HNFs and nanopaper.

In this work, HNFs were prepared by a polymerization-induced self-assembly method, where 5 g of $CaCl_2$ was added and dissolved in 100 mL of NMP at 100 °C in a reactor under nitrogen atmosphere. Then the reaction system was cooled down to 0–10 °C using an ice water bath. *p*-Phenylene diamine (PPD) and the third monomer APBZ (the total concentration 0.2 mol L^{-1}) were added and dissolved in NMP solution under stirring. The addition ratio of APBZ in amine monomer was 20%, 40%, 50%, 60% and 80%. Finally, 4.089 g of terephthaloyl chloride (TPC) was added subsequently into the system and the reaction started under high speed stirring. The reaction was stopped when the Weissenberg effect happened (Fig. S1, ESI†). A certain amount of HAP gel was taken out and diluted by excess NMP. Then, the diluent was added slowly into plenty of deionized water under strong shear to obtain the heterocyclic aramid nanofiber (HNF) dispersion. All the dispersions are uniform and stable, showing different colours with different APBZ addition ratios (Fig. S2, ESI†).

The results of the FTIR characterization of HAP are shown in Fig. 2. In addition to the typical peaks of aromatic polyamides,[33] the occurrence of peaks at 1600 cm^{-1} and 1422 cm^{-1} represents the C=N stretching vibration of the imidazole ring and the bending vibration absorption of the imidazole ring, respectively,[34,35] which indicates successful participation of APBZ in the copolymerization. The molecular weights of the obtained HNFs are shown in Table S1 (ESI†). All the molecular weights are more than ten thousand Dalton and varied with APBZ addition ratio, which is similar to the copolymerization in the DMAc/LiCl solvent system.[36] This not only demonstrates the availability of NMP/$CaCl_2$ for copolymerization of APBZ in PPTA, but also ensures the excellent properties of HNFs such as thermal stability which can also be inferred from the TGA data as shown below (Fig. 5b).

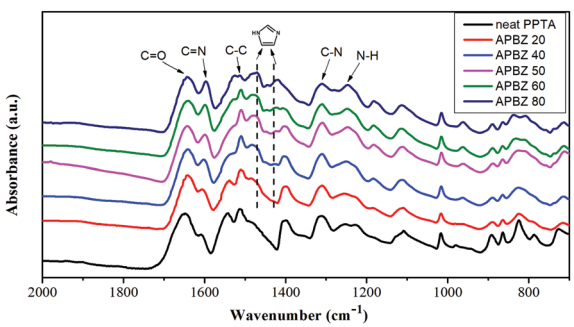

Fig. 2 The FTIR spectra of HAP with different APBZ addition ratios.

The HNF structures we obtained are shown in Fig. 3. According to the TEM results, PPTA and HAP can self-assemble into nanofibrillar structures, which confirms the feasibility of the polymerization-induced self-assembly method without polyoxyethylene ether as interfacial isolation. However, APBZ has a significant influence on the morphology of the formed nanostructure. Without APBZ addition, ANF is uniformly dispersed with a diameter of about 60 nm and extremely high length to diameter ratio. As the proportion of APBZ increases, the HNF morphology gradually changes from a fibrous structure to ribbon-like aggregation. In the process of nanofiber formation, NMP/$CaCl_2$ has a solvent isolation effect for aramid molecular chains. When the amount of APBZ added is low, the balance of solvent isolation effect and intermolecular interactions induced the formation of fibrillation in the nanoscale. After the addition ratio of APBZ up to 60%, agglomeration can be observed obviously. It is speculated that the heterocyclic monomer destroyed the planar conjugated molecular chain structure of PPTA and the molecular chain gradually begins to warp and agglomerate, resulting in changes in the micro–nano structure. From a macro perspective, HNFs can be uniformly dispersed in water. The colour of the dispersion becomes darker as the addition ratio of APBZ increases, which also indicates the success of copolymerization.

The preparation process of HNF paper shown in Fig. 1 is easy and effective. Excess water of HNF dispersion was filtered out by sintered discs with the help of vacuum. Finally, the wet paper was put in two smooth and flat glass plates and dried in a vacuum oven (<100 Pa) at 60 °C for 48 h. ANF paper was prepared for comparison through the same process as described above but without APBZ addition.

As is shown in Fig. 4(a), HNF paper with a thickness of around 30 μm has a homogeneous appearance with high transparency. The SEM image in Fig. 4(b) indicates that the surface of HNF paper is uniform and smooth without any obvious defects. Micro-level observations reveal the disappearance of the interface between most nanofibers. On the contrary, the obtained ANF paper through the same preparation process is less uniform with more defects such as pores at the

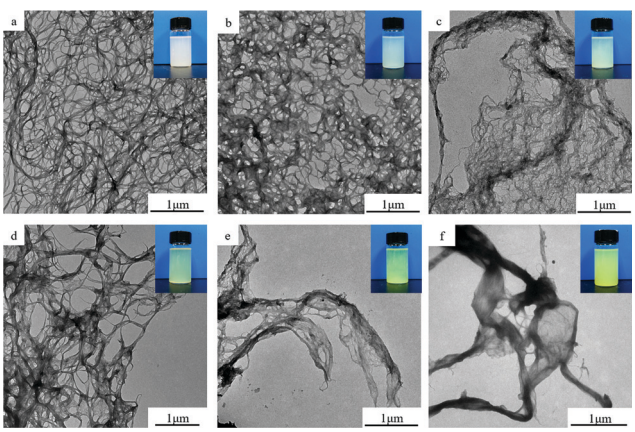

Fig. 3 TEM images of HNF with different APBZ addition ratios: (a) 0%, (b) 20%, (c) 40%, (d) 50%, (e) 60%, and (f) 80%.

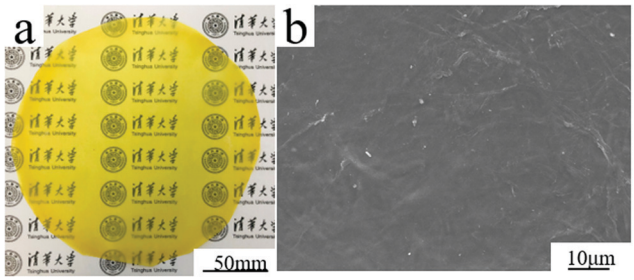

Fig. 4 (a) The appearance of HNF paper; (b) SEM image of the paper surface (APBZ addition ratio 50%).

microscale (Fig. S3, ESI†). This difference between HNF and ANF papers implies the strong intermolecular interactions between HNFs during the drying process.

In order to evaluate the performance of HNF paper, tensile strength, thermal stability and electrical breakdown tests were performed subsequently. As shown in Fig. 5(a), The stress–strain curve of HNF paper with different APBZ addition ratios demonstrated that the tensile strength (TS) has been significantly improved compared with ANF paper. When the APBZ addition ratio is 50%, the TS of HNF paper reaches a maximum value of 203.5 MPa. At the same time, the elongation at break (EB) has also been greatly improved to 19% due to the addition of nonlinear comonomer, indicating that the heterocyclic molecular structure facilitates the strengthening and toughening of the aramid nanofiber paper.

Fig. 5(b) shows the TGA curve of aramid paper. It can be seen that the thermal stability of HAP is almost the same as that of pure PPTA fiber and the thermal decomposition temperature (T_d) is about 550 °C. In addition, with the increase of the APBZ addition ratio, the residual mass of the samples also suggests an increasing trend, which confirms the high temperature resistance of the copolymer. At high temperature, compared with the benzene ring, benzimidazole has a higher residual mass and thermal stability due to its stable aromatic ring structure.[37]

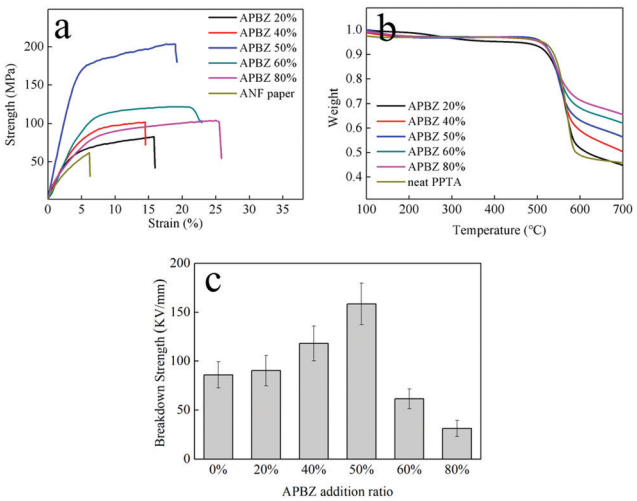

Fig. 5 (a) The stress–strain curves of HNF paper and ANF paper. (b) The TGA curves of HNF and neat PPTA. (c) EBS of HNF paper and ANF paper.

Table 1 Comparison of ANF paper, HNF paper and Nomex® 412

Type	Thickness/ μm	Density/ (g m^{-2})	EBS/ (kV mm^{-1})	TS/MPa	EB/%	T_d/°C
ANF paper	47	48.5	90	75.5	5.5	550
HNF paper	30	42.1	158	203.5	19.0	550
Nomex® 412	60	41.5	15	58.7	17.0	420

In this work, the residual mass of HNF with 20% APBZ addition ratio improvement is not obvious, but the change of residual mass of the other HNFs followed this rule which indicates that the more benzimidazole segments, the more residual mass.[38,39]

As shown in Fig. 5(c), heterocyclic copolymerization can significantly increase the electrical breakdown strength (EBS) value compared with that of ANF paper due to the uniform and smooth structure. With the increase of APBZ addition ratio, the EBS of HNF paper also increases first and then decreases with the highest value of 158 kV mm^{-1} at 50% APBZ addition ratio. The EBS values are sharply higher than the commercial products such as 15 kV mm^{-1} of Nomex® 412 paper as shown in Table 1. The TEM images in Fig. 3 illustrate that HNFs are more likely to agglomerate when the APBZ addition ratio is high, resulting in lower density and declining electrical insulation. Table 1 compares the performance of ANF paper, HNF paper and Nomex® 412, implying that the introduction of APBZ (addition ratio $\leq$50%) leads to a comprehensive performance improvement of aramid nanofiber paper, especially in mechanical and insulation properties. For HNF paper, the smaller thickness has a higher surface density and ultra-high properties, which also reveals its compact structure and great enhancement effect. Importantly, with excellent mechanical strength and toughness, HNF paper has the best insulation in the field of aramid paper by far.

In conclusion, heterocyclic aramid nanofibers and the paper-based material were prepared for the first time by copolymerization in this study. The mechanical, electrical, and thermal stability properties of HNF paper were characterized in detail. The effects of heterocyclic monomers on the micro–nano structure and properties of aramid paper were evaluated. The whole preparation process did not use any additives, NMP/$CaCl_2$ was proved effective for HAP polymerization and the characteristics of the obtained nanofibers and the performance of the HNF paper were impressive. It was found that compared with ANF paper, the HNF paper maintains high heat resistance and its mechanical properties and electrical insulation properties have been significantly improved, which makes up for the brittleness of ANF papers. All the results demonstrated that copolymerization with a heterocyclic monomer is a good way to improve the performance of aramid nanofibers and is easy to implement for industrial production, which provides new ideas for the research of copolymerized aromatic polyamides. Through this study, HNF paper is expected to be used in broader application ranges and higher performance requiring cases.

Conflicts of interest

There are no conflicts to declare.

Acknowledgements

This work was financially supported by the Major Program for Scientific and Technological Innovation in Shandong Province (No. 2019TSLH0109) and the funding of Tsinghua University-Chambroad Research Center for High Performance Polymers.

Notes and references

1 G. Srinivasan and D. Reneker, *Polym. Int.*, 1995, **36**, 195–201.
2 J. Yao, J. Jin, E. Lepore, N. M. Pugno, C. Bastiaansen and T. Peijs, *Macromol. Mater. Eng.*, 2015, **300**, 1238–1245.
3 M. Yang, K. Cao, L. Sui, Y. Qi, J. Zhu, A. Waas, E. Arruda, J. Kieffer, M. Thouless and N. A. Kotov, *ACS Nano*, 2011, **5**, 6945–6954.
4 S. Ifuku, H. Maeta, H. Izawa, M. Morimoto and H. Saimoto, *RSC Adv.*, 2014, **4**, 40377–40380.
5 H. C. Yan, J. L. Li, W. T. Tian, L. Y. He, X. L. Tuo and T. Qiu, *RSC Adv.*, 2016, **6**, 26599–26605.
6 C. Nie, Z. Peng, Y. Yang, C. Cheng, L. Ma and C. Zhao, *J. Hazard. Mater.*, 2016, **318**, 255.
7 Y. Li, E. Wong and Z. Mai, *J. Membr. Sci.*, 2019, **592**, 117396.
8 J. U. Lee, B. Park, B. S. Kim, D. R. Bae and W. Lee, *Composites, Part A*, 2016, **84**, 482.
9 J. Lin, S. H. Bang, M. H. Malakooti and H. A. Sodano, *ACS Appl. Mater. Interfaces*, 2017, **9**, 11167.
10 J. Q. Zhu, W. X. Cao, M. L. Yue, Y. Hou, J. C. Han and M. Yang, *ACS Nano*, 2015, **9**, 2489.
11 Z. Ma, S. Kang and J. Ma, *ACS Nano*, 2019, **13**, 7578.
12 S. R. Kwon, J. Harris, T. Zhou, D. Loufakis, J. G. Boyd and J. L. Lutkenhaus, *ACS Nano*, 2017, **11**, 6682.
13 W. Cao, L. Yang, X. Qi, Y. Hou, J. Zhu and M. Yang, *Adv. Funct. Mater.*, 2017, **27**, 1701061.
14 J. Lyu, Z. Liu, X. Wu, G. Li, D. Fang and X. Zhang, *ACS Nano*, 2019, **13**, 2236.
15 B. Yang, L. Wang and M. Zhang, *Adv. Funct. Mater.*, 2020, 2000186.
16 S. O. Tung, S. L. Fisher, N. A. Kotov and L. T. Thompson, *Nat. Commun.*, 2018, **9**, 4193.
17 L. Y. He, T. Qiu, C. J. Xie and X. L. Tuo, *J. Appl. Polym. Sci.*, 2018, **135**, 46697.
18 C. Nie, Z. Peng, Y. Yang, C. Cheng, L. Ma and C. Zhao, *J. Hazard. Mater.*, 2016, **318**, 255–265.
19 Y. Li, E. Wong and Z. Mai, *J. Membr. Sci.*, 2019, **592**, 117396.
20 Z. Ma, S. Kang, J. Ma, L. Shao, A. Wei, C. Liang and Z. Ji, *ACS Nano*, 2019, **13**, 7578–7590.
21 W. T. Tian, T. Qiu, Y. F. Shi, L. Y. He and X. L. Tuo, *Mater. Lett.*, 2017, **202**, 158–161.
22 R. M. Versteegen, R. P. Sijbesma and E. W. Meijer, *Macromolecules*, 2005, **38**, 3176–3184.
23 T. Goto, M. Maeda and S. Hibi, *J. Appl. Polym. Sci.*, 1989, **37**, 867–875.
24 Y. Wang, X. Zhang and D. Zhang, *et al.*, *Polym. Int.*, 2014, **63**, 727–732.
25 A. Jalali, A. Shockravi and V. Vatanpour, *et al.*, *Microporous Mesoporous Mater.*, 2016, **228**, 1–13.
26 A. Leal, J. M. Deitzel and J. W. Gillespie, *Compos. Sci. Technol.*, 2007, **67**, 2786–2794.
27 L. Luo, J. Yao and X. Wang, *Polymer*, 2014, **55**, 4258–4269.
28 K. Perepelkin, N. Machalaba and V. Kvartskheliya, *Fibre Chem.*, 2001, **33**, 105–114.
29 L. Luo, Y. Wang, Y. Dai, Y. Yuan, C. Meng, Z. Cheng and X. Y. Liu, *J. Mater. Sci.*, 2018, **53**, 13291–13303.
30 F. Xing, M. Zhang, Z. Wang, G. Sun, H. Niu and D. Z. Wu, *RSC Adv.*, 2019, **9**, 33664–33673.
31 T. I. Bair, P. W. Morgan and F. L. Kiillian, *Macromolecules*, 1977, **10**, 1396.
32 E. Chodkowski, J. Mackowiak, W. Kozlowski and H. Orzechowska, *Polimery*, 1971, **16**, 514.
33 G. D. Litovchenko, T. S. Sokolova, A. V. Volokhina, G. I. Kudryavtsev and S. P. Papkov, *J. Appl. Spectrosc.*, 1974, **20**, 345–348.
34 S. Wang, H. Zhou, G. Dang and C. Chen, *J. Polym. Sci., Part A: Polym. Chem.*, 2009, **47**, 2024–2031.
35 V. Arjunan, A. Raj, C. Mythili and S. Mohan, *J. Mol. Struct.*, 2013, **1036**, 326–340.
36 L. Chen, Z. M. Hu and B. S. Gao, *Adv. Mater. Res.*, 2011, **146**, 470–474.
37 Y. Zhuang, X. Liu and Y. Gu, *Polym. Chem.*, 2012, **3**, 1517.
38 L. Luo, Y. Yuan and Y. Dai, *Mater. Des.*, 2018, **158**, 127–135.
39 L. Luo, Y. Wang and Y. Dai, *J. Mater. Sci.*, 2018, **53**, 13291–13303.

